ON THE DYNAMICAL EVOLUTION OF A FRAGMENTATION IN THE MOLNIYA REGIME

E.M. Alessi(1) **and Alessandro Rossi**(2)

(1)*Istituto di Matematica Applicata e Tecnologie informatiche, Consiglio Nazionale delle Ricerche, 20133 Milano, Italy, Email: elisamaria.alessi@cnr.it*

(2)*Istituto di Fisica Applicata, Consiglio Nazionale delle Ricerche, 50019 Sesto Fiorentino (FI), Italy , Email: a.rossi@ifac.cnr.it*

ABSTRACT

Motivated by need of improving the current mitigation measures and the catalogue of orbiting objects, this work analyzes the orbital distribution, at different timescales, of the fragments that can originate from a well-defined explosion in Molniya orbit. The analysis will focus first on the behavior of mean anomaly and longitude of the ascending node and then in geocentric right ascension and declination. In the latter case, a specific machine learning clustering method is applied to identify the regions where it would be more likely to observe objects. As expected, the dynamics of the cloud is much slower compared to the one in LEO, and, in principle, the nominal orbit of the parent body could be identified even after 5-10 years since the event. The most favorable declination range to get useful observations up to 10 years after a fragmentation event is identified too.

Keywords: Molniya; fragmentation; HEO; clustering.

1. INTRODUCTION

The Molniya orbit is a highly elliptical orbit (HEO) at the critical inclination, thus with a frozen argument of pericenter. It was exploited to cover the Soviet/Russian territory, and it is paradigmatic given the richness of the associated dynamics. Following [1], the three series of Molniya satellites were operational in the timeframe 1965-2008.

In this work, we simulate the orbital evolution of a cloud of fragments derived from an explosion in such orbital regime, to evaluate possible clusterings that can be observed by dedicated campaigns. The main motivation is the improvement of the current knowledge of the space debris population in orbital regimes different from LEO, with special emphasis on the behavior in HEO. The simulations analyzed here are the same presented in [2], but while there the focus was more on the role of the initial change in velocity due to the explosion and of the orbital perturbations, here the analysis is refined and extended to highlight the clustering effect throughout the years. The data used to this end consist in geocentric right ascension and declination, as they can provide a direct indication on where it would be more efficient to observe. The different phases of the cloud evolution will be described to compare with the behavior in LEO, and also to show the time limit within which it is possible to reconstruct the initial event.

2. METHODOLOGY

We simulated the breakup of 3 different spacecraft due to an explosion at the pericenter and the apocenter at 2 different epochs for each case. The initial conditions for the explosions that we simulated are shown in Table 1, while the corresponding evolution for the nominal orbit is shown in Fig. 1. They were chosen according to historical TLE series of Molniya satellites [3, 4], paying attention to consider cases where the orbital perturbations may play a different role. The mass of the fragmented object is assumed to be 1250 kg for cases 1,2, 1500 kg for cases 3,4, and 1800 kg for cases 5,6, according to [5].

The simulation of the clouds of fragments and their evolution was carried out by means of a software based on the NASA BreakUp Model EVOLVE 4.0 [6], as implemented in the SDM 4.0 software suite [7, 8]. The initial number of fragments larger than 10 cm is 253 for the 12 cases simulated. Once the distribution of the fragments, in terms of area and mass, is produced, the model assumes an isotropic distribution of the velocity increment vectors ($\Delta\mathbf{v}$) of the fragments. The orbit of each fragment larger than 10 cm is then computed by adding the $\Delta\mathbf{v}$ to the Cartesian state vector of the fragmented object and is then propagated up to 50 years by using the the Fast Orbit Propagator (FOP) [7, 8], which is an accurate, long-term orbit predictor, based on the Long-term Orbit Predictor (LOP) [9].

FOP relies on a singly-averaged formulation, that accounts for geopotential harmonics (up to degree and order 5), lunisolar gravitational perturbations, atmospheric

Proc. 9th European Conference on Space Debris, Bonn, Germany, 1–4 April 2025, published by the ESA Space Debris Office
Editors: S. Lemmens, T. Flohrer & F. Schmitz, (http://conference.sdo.esoc.esa.int, April 2025)

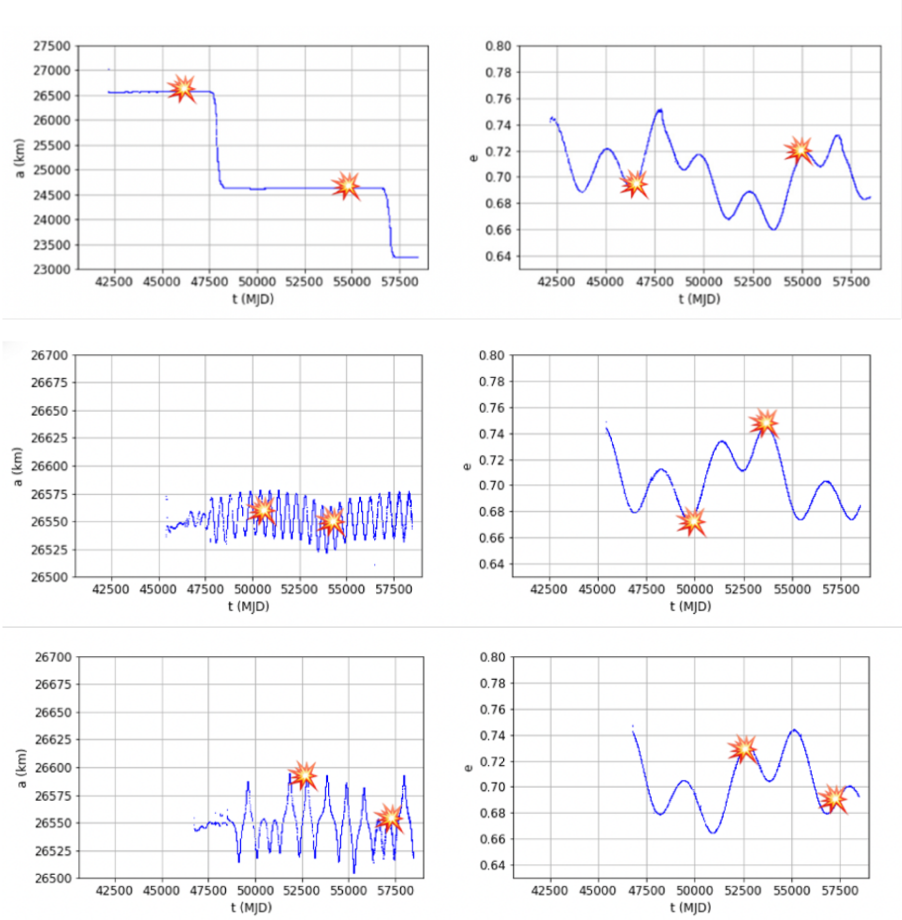

Figure 1. Nominal evolution in semi-major axis (left) and eccentricity (right) of TLE used to choose the initial conditions for the simulations (the explosions in the plots). Top: cases 1-2; middle: cases 3-4; bottom: cases 5-6.

Table 1. Osculating initial conditions for the explosion simulated at t_0. Units: km, deg.

case	t_0	a	e	i	Ω	ω	M
1a	1985/08/25 11:26	26573,03	0,691	63,22	208,84	260,40	0
1b	1985/08/25 11:26	26573,03	0,691	63,22	208,84	260,40	180
2a	2009/06/26 11:18	24630,39	0,717	63,36	352,48	252,40	0
2b	2009/06/26 11:18	24630,39	0,717	63,36	352,48	252,40	180
3a	1994/09/25 08:20	26548,75	0,672	63,90	200,86	263,50	0
3b	1994/09/25 08:20	26548,75	0,672	63,90	200,86	263,50	180
4a	2005/10/16 05:19	26595,83	0,745	62,76	11,59	280,52	0
4b	2005/10/16 05:19	26595,83	0,745	62,76	11,59	280,52	180
5a	2003/06/07 13:58	26607,34	0,730	62,93	333,44	256,91	0
5b	2003/06/07 13:58	26607,34	0,730	62,93	333,44	256,91	180
6a	2016/01/13 19:50	26524,67	0,690	64,03	81,69	277,05	0
6b	2016/01/13 19:50	26524,67	0,690	64,03	81,69	277,05	180

Table 2. The number of fragments larger than 10 cm after 5, 10, 15, 20, 25, 50 years.

case	5	10	15	20	25	50
1a	108	88	86	85	84	82
1b	119	102	98	97	97	91
2a	173	43	34	31	28	18
2b	138	98	96	94	94	80
3a	236	232	232	232	232	199
3b	237	219	205	202	202	165
4a	251	251	251	243	227	200
4b	183	180	178	168	157	135
5a	253	252	252	252	250	227
5b	216	191	190	190	188	164
6a	253	253	208	174	169	50
6b	248	221	187	164	164	102

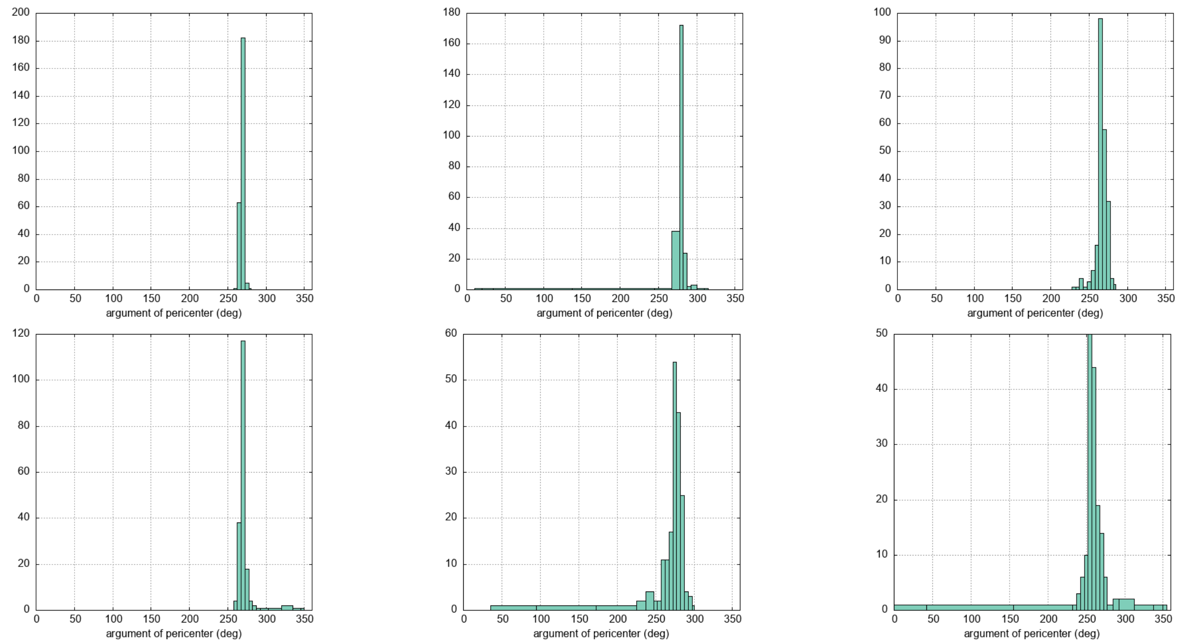

Figure 2. Distribution in ω (5°-width) after 15 (left), 30 (middle) and 50 years (right) for cases 5a (top) and 5b (bottom).

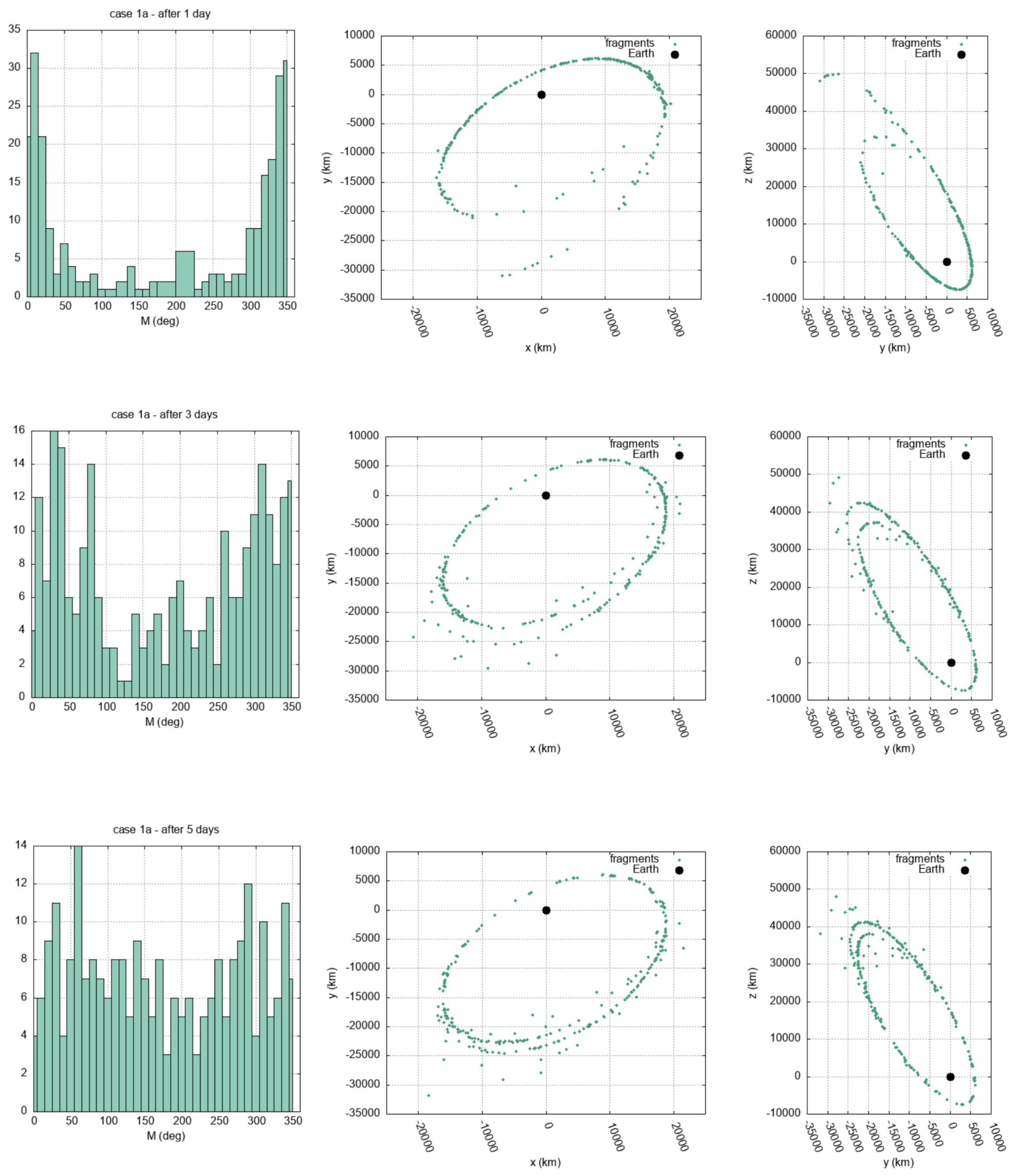

Figure 3. Evolution of the cloud for case 1a after 1 day (top), 3 days (middle), 5 days (bottom). The breakup occurred at the pericenter. The plots on the left show the number of fragments in bins of mean anomaly (10°-width).

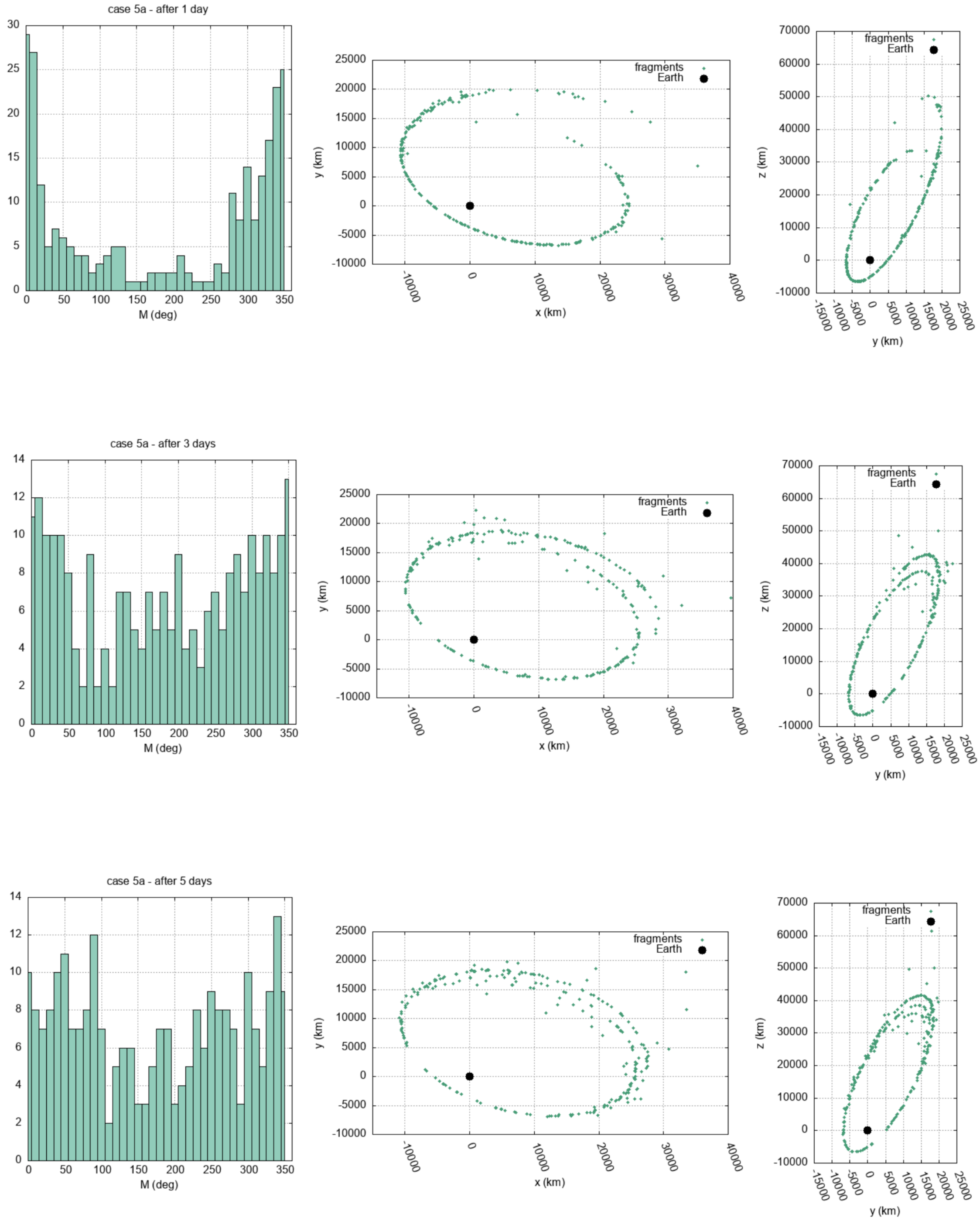

Figure 4. Evolution of the cloud for case 5a after 1 day (top), 3 days (middle), 5 days (bottom). The breakup occurred at the pericenter. The plots on the left show the number of fragments in bins of mean anomaly (10°-width).

drag and solar radiation pressure (SRP), including shadows. For tesseral resonant effects (located at specific values of semi-major axis, where there exists a commensurability between the satellite's mean motion and the Earth's rotation rate), a partial averaging procedure is applied to retain only the long-periodic perturbations associated with these harmonics. The positions of the Moon and the Sun, which are held constant during the averaging process, are determined by means of accurate analytical ephemerides. The SRP effect is represented by the cannonball model, accounting also for shadowing intervals. The shadows are modeled as solar occultations, with a cylindrical model. The algorithm assumes that the Sun is a point at infinity and that the spacecraft and the Sun are frozen during the occultation. The atmospheric drag is applied for altitudes below 1500 km, adapting the Jacchia-Roberts density model assuming an exospheric temperature of 1000 K and a variable solar flux at 2800 MHz (obtained by means of a Fourier analysis of data corresponding to the interval 1961-1992). To average the disturbing accelerations associated with solar radiation pressure and atmospheric drag, a standard 8th-order Gaussian quadrature method is used. The numerical integrator is a multi-step, variable step-size and order integrator.

3. RESULTS

In [2], we showed that:

- the atmospheric drag can be relevant if it is for the nominal orbit or when the initial Δv occurs at the apocenter lowering the pericenter altitude (see cases 4 and 5) [1];
- after 50 years the cloud has not reentered fully (see Tab. 2 - last column) in any of the cases simulated;
- the eccentricity can start exhibiting a meaningful deviation from the one of the nominal orbit after about 15 years;
- the initial Δv and the third-body perturbation are not as much important as to move significantly the inclination of the orbit of the fragments with respect to the one of the parent body (at least for the initial conditions considered here).

Following [10], we can distinguish two main phases after the breakup event. After the initial ellipsoid is formed, we have first a randomization in mean anomaly M, driven by the difference in a and e due to the explosion's Δv. The fragments distribute along the orbit, being the Earth's monopole dominant in this phase, and the cloud assumes a toroid shape. Later on, the oblateness effect takes over and the longitude of the ascending node Ω and the argument of pericenter ω randomize. The cloud is spread into a shell around the altitude of the fragmentation. This description is usually considered for fragmentations in Low Earth Orbit.

For the fragmentations we simulated, it turns out that the randomization in M and Ω is 3 times and 10 times, respectively, slower than a typical fragmentation in LEO. Given the critical inclination, a randomization in ω does not take place, but we can observe a dispersion (approximately up to about 30° with respect to the nominal value) in decades. See Fig. 2 for two examples.

Here, we consider that a given orbital element has randomized when in the corresponding distribution we cannot distinguish any characteristic trend or peak. For M, if the breakup has happened at the pericenter, the fragments distribute along the whole orbit in less than 5 days, as shown in Figs. 3-4. If it has occurred at the apocenter, it can take 3 weeks, see Figs. 5-6.

Concerning the behavior in Ω, considering the cases where the atmospheric drag is not dominant (i.e., excluding cases 1,2) in 20 years the orbit of the fragment can take any value of Ω (see Fig. 7). It is true that at 20 years we can notice some peaks, but they correspond to a number of fragments not significantly different with respect to those associated with other values of Ω.

The above considerations were translated in geocentric right ascension α and declination δ and a clustering method was applied to identify groups of objects that can be observed more easily. Assuming that a given fragmentation occurred a few years ago, we applied the Mean Shift method, borrowed from the Python open source library `scikit-learn` [11], to the $(\alpha, \delta : \delta > 0)$ values of the clouds corresponding to years 1 to 20 since the breakup event for all the cases displayed in Table 1. The output of the method are the clusters identified in terms of members of the cluster, but also in terms of centroid. We considered that the clustering was good if the set contains at least 5 objects, with a distance to the centroid less than 10°. These parameters can be adjusted according to the observation strategy (e.g., [12]). In Fig. 8, we show two examples of output.

For cases 1-2 where the drag plays an important role, the clustering method is effective up to 5 years, later we cannot recognize specific sets of fragments. For the other cases, instead, we can see clusters complying with the above setting, up to 20 years.

Figure 9 shows the location of the centroids at the given year since the fragmentation, for all the cases. Up to 5 years, they follow the nominal orbit: looking to the top left plot we can see 4 different trends, that are due to the different initial value of Ω (see Table 1). After 10 years most of the clusters are located at a declination in the range $[50° : 65°]$ spanning the whole range in right ascension, although we can see some also at lower values of δ. Notice that, as can be seen also from the figures shown in [2], the fragments at the highest declination are

[1] The significant drop in the number of fragments after 50 years for case 6a is due to an increase in eccentricity that takes place after 30 years since the event.

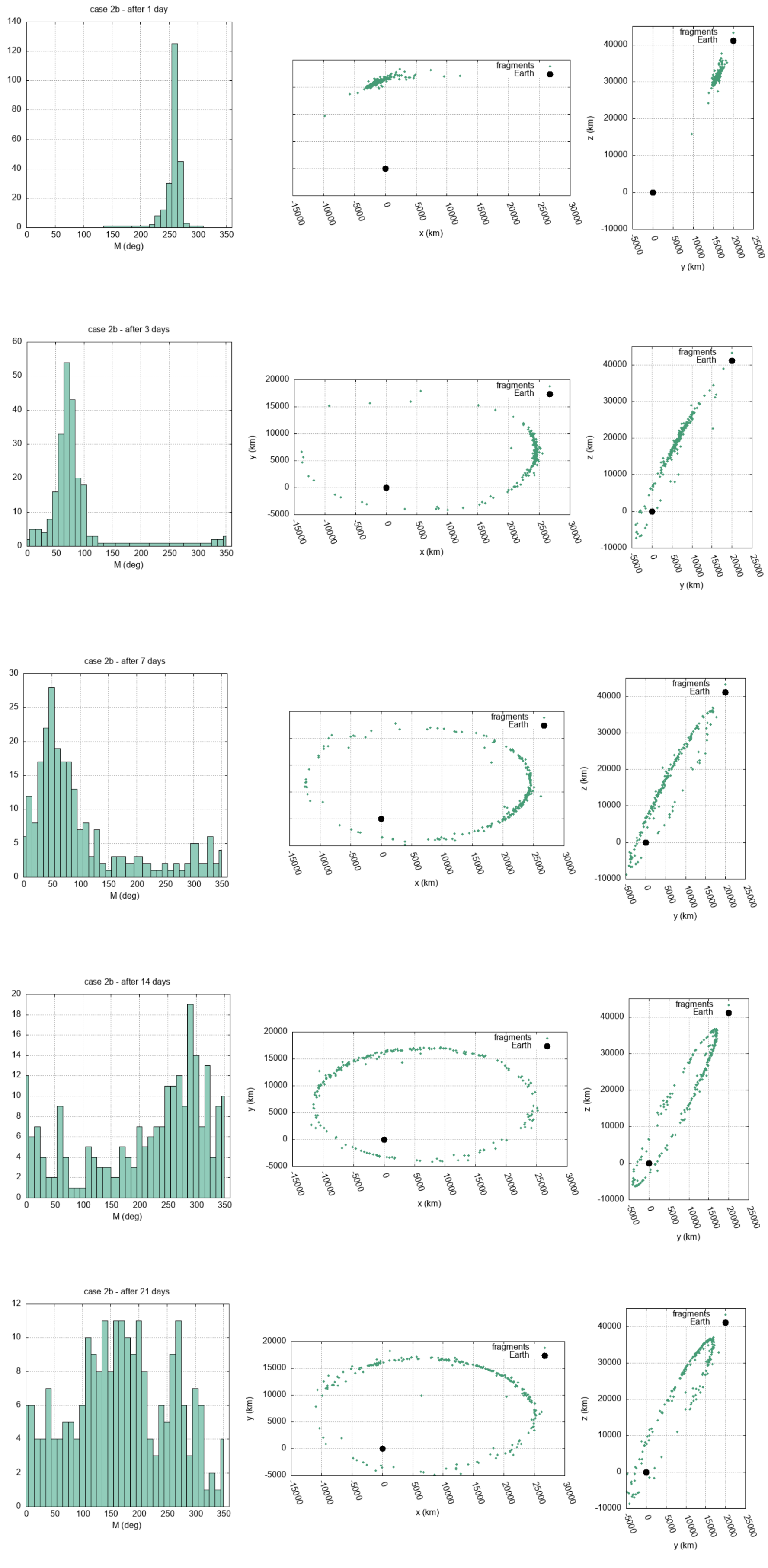

case 2b - after 1 day
M (deg)
fragments
Earth
x (km)
z (km)
y (km)
case 2b - after 3 days
M (deg)
fragments
Earth
y (km)
x (km)
z (km)
y (km)
case 2b - after 7 days
M (deg)
fragments
Earth
x (km)
z (km)
y (km)
case 2b - after 14 days
M (deg)
fragments
Earth
y (km)
x (km)
z (km)
y (km)
case 2b - after 21 days
M (deg)
fragments
Earth
y (km)
x (km)
z (km)
y (km)

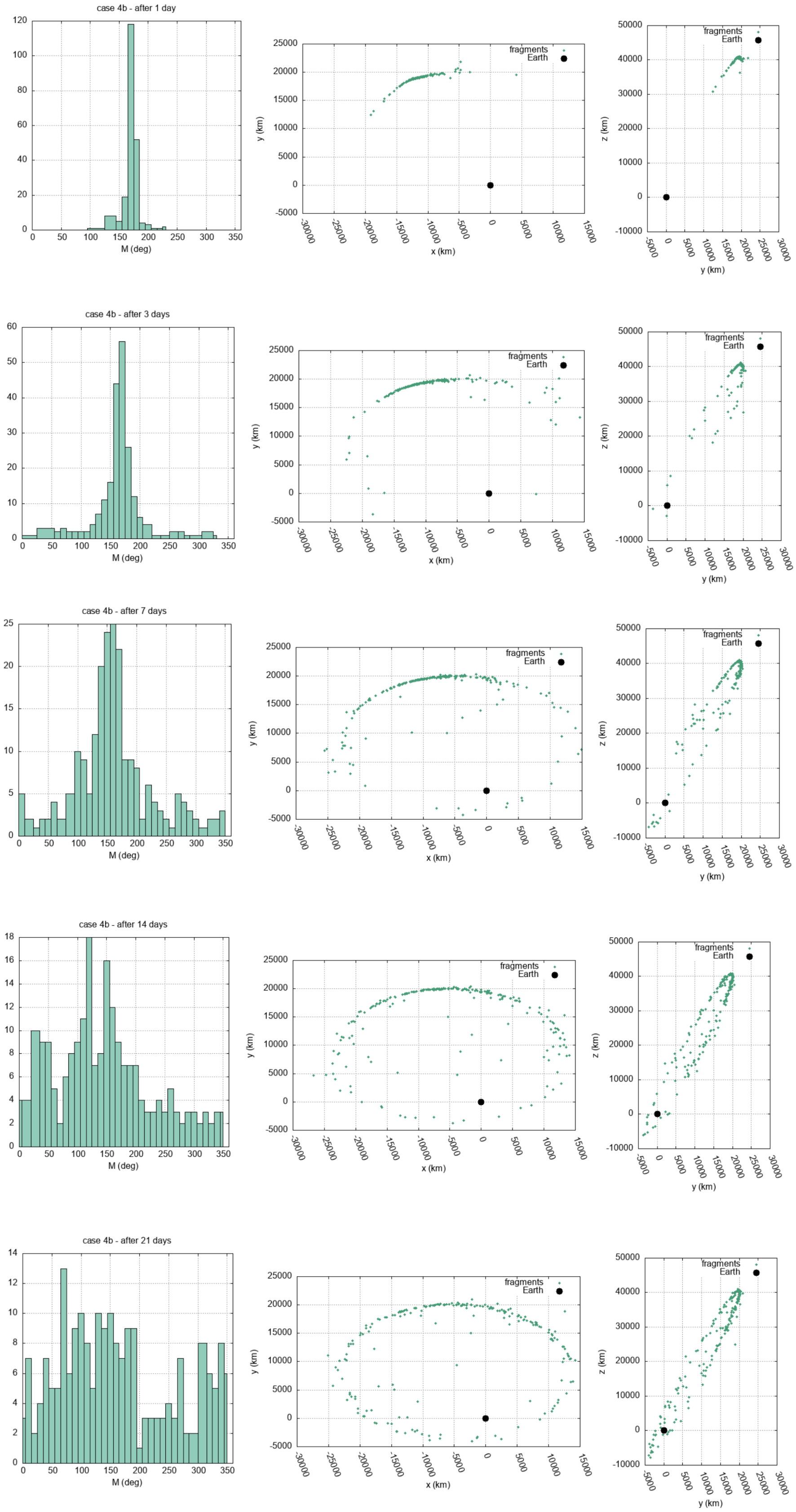

Figure 6. Evolution of the cloud for case 4b after 1 day, 3, 7, 14 and 21 days (from top to bottom). The breakup occurred at the apocenter. The plots on the left show the number of fragments in bins of mean anomaly (10°-width).

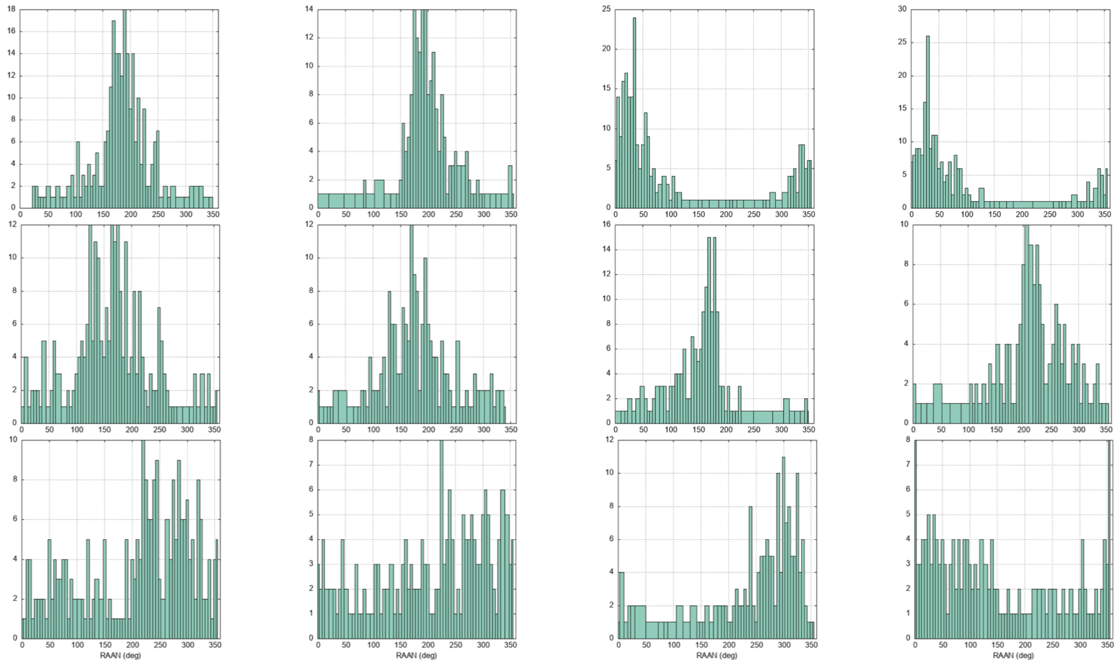

Figure 7. Distribution in Ω (5°-width) after 10 (top), 20 (middle) and 25 years (bottom) for cases 5a, 5b, 6a, 6b (left to right).

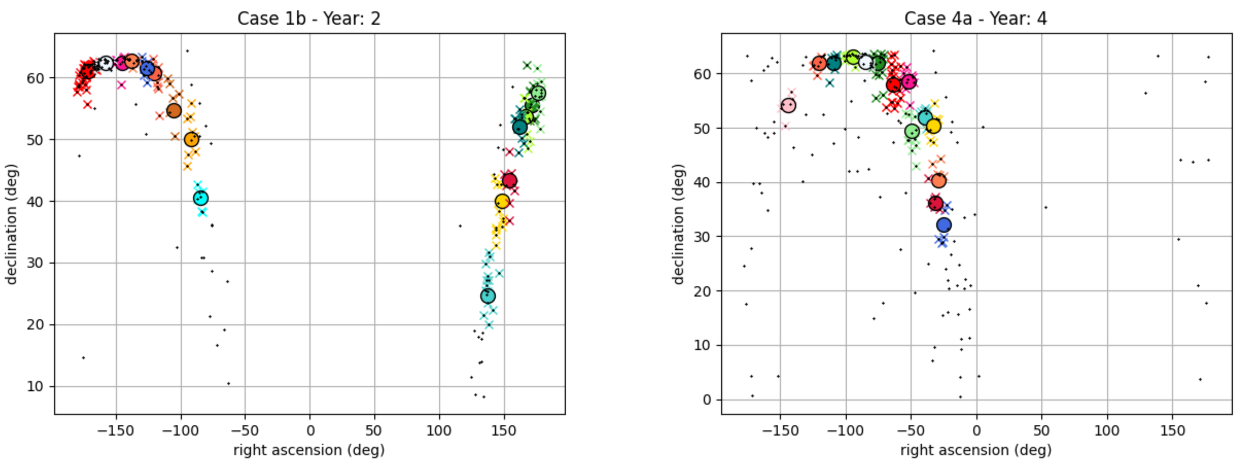

Figure 8. Clusters (denoted by a different color) found for case 1b after 2 years since the breakup (left) and for case 4a after 4 years (right). The centroid of the given cluster is depicted with a larger empty circle. The black dots are fragments that are not linked to any cluster.

orbiting at the apocenter, while in general the clusters corresponding to $\delta > 40°$ have a mean anomaly in the range $[50° : 300°]$[2]. In other words, after several years we still have fragments orbiting at low declinations, but the clusters are detected at higher values because the fragments are slower and spend more time there.

4. CONCLUSIONS

In this work, we have analyzed the behavior of illustrative fragmentations in the Molniya regime, so that an observational campaign in the region could be optimized. Being the dynamics slow, the fragments orbit in the neighborhood of the orbit of the parent body for a few years. This could facilitate the cataloguing of the corresponding objects when the fragmentation has just happened, where 'just' refers to few weeks. On the other hand, it could be possible to identify the parent body after 5-10 years since the explosion, if enough fragments are observed on a characteristic curve in (α, δ) of a Molniya orbit. In general, the main suggestion is to focus on declinations higher than 50°.

In the future, it would be worth to perform a more systematic study changing the initial value of the ascending node and the mean anomaly to better characterizing the possible deviation in inclination of the orbit of the fragments.

ACKNOWLEDGMENTS

The work was performed under the ASI Contract "Detriti Spaziali - Supporto alle attività IADC e SST 2023-2025".

REFERENCES

1. Buzzoni A., et al., (2020). Spectrophotometric and dynamical properties of the Soviet/Russian Constellation of Molniya Satellites. *Journal of Space Safety Engineering*, **73**, 255–261.
2. Alessi E.M., Rossi A., (2024). Orbital evolution of a Molniya fragmentation. *International Astronautical Congress 2024*, Milan, Italy, paper IAC-24,A6,IP,71,x89275.
3. Alessi E.M., et al., (2021). Dynamical properties of the Molniya satellite constellation: Long-term evolution of orbital eccentricity. *Acta Astronautica*, **179**, 659–669.
4. Daquin J., et al., (2021). Dynamical properties of the Molniya satellite constellation: long-term evolution of the semi-major axis. *Nonlinear Dynamics*, **105**, 2081–2103.
5. NASA Space Science Data Coordinated Archive, https://nssdc.gsfc.nasa.gov/
6. Johnson N.L., et al., (2021). NASA's new breakup model of evolve 4.0. *Advances in Space Research*, **28**, 1377–1384.
7. Anselmo L., et al., (1996). Study on long term evolution of Earth orbiting debris. *ESA/ESOC contract No. 10034/92/D/IM(SC).*
8. Rossi A., et al., (2009). The new space debris mitigation (SDM 4.0) long term evolution code. *Proceedings of the 5th European Conference on Space Debris*, Darmstadt, Germany, Paper ESA SP-672.
9. Kwok J.H., (1986). The long-term orbit prediction (LOP). *JPL Technical Report EM 312/86-151.*
10. Jehn R., (1991). Dispersion of debris clouds from In-orbit fragmentation events, *ESA Journal*, **1**, 63–77
11. Pedregosa F., et al., (2011). Scikit-learn: Machine Learning in Python, *Journal of Machine Learning Research*, **12**, 2825–2830.
12. Rossetti M., et al., (2025). Characterization of a fragmentation in Highly Elliptical Orbit via optical multi-observatory survey strategy. *Aerospace*, **123**, 81.

[2]Recall that

$$\delta = z/\sqrt{x^2 + y^2} = \sin(\omega + \nu) \sin i / \sqrt{1 - (\sin(\omega + \nu) \sin i)^2}$$

, being ν the true anomaly.

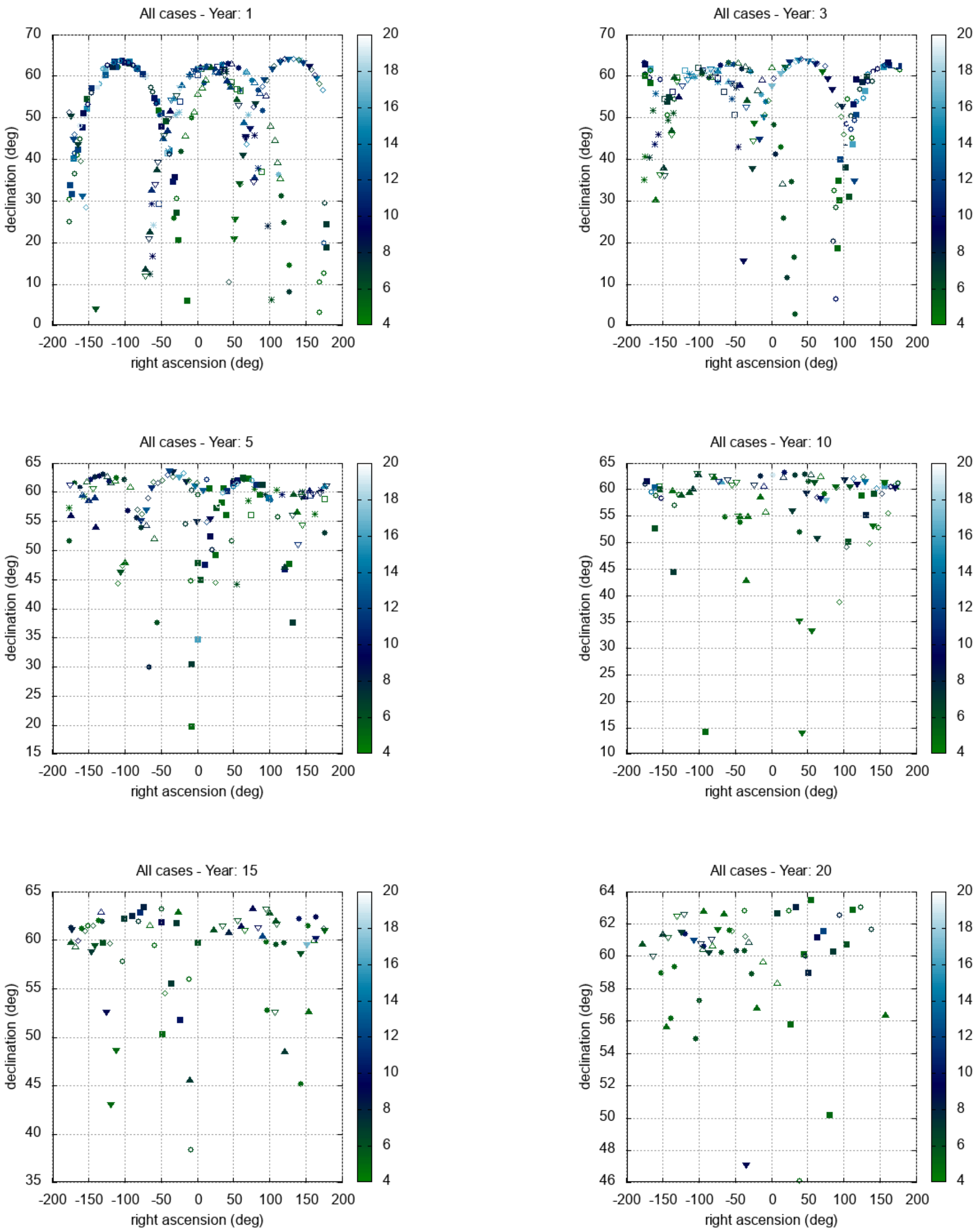

Figure 9. Centroids of all the clusters identified at the given year (from top left to bottom right 1, 3, 5, 10, 15, 20) since the breakup. The color represents the number of members of the corresponding cluster, the different marker represents the different case (1-12).